19th INTERNATIONAL CONGRESS ON ACOUSTICS
MADRID, 2-7 SEPTEMBER 2007

THE EFFECTS OF INTERNAL RESONANCES IN VIBRATION ISOLATORS UNDER ABSOLUTE VELOCITY FEEDBACK CONTROL

PACS: 43.40.Vn

Yan, Bo; Brennan, Mike; Elliott, Steve; Ferguson, Neil
Institute of Sound and Vibration Research, University of Southampton, Southampton, SO17 1BJ, United Kingdom; by@isvr.soton.ac.uk; mjb@isvr.soton.ac.uk; sje@isvr.soton.ac.uk; nsf@isvr.soton.ac.uk;

ABSTRACT
Conventional vibration isolators are usually assumed to be massless for modelling purposes, which tends to overestimate the isolator performance because the internal resonances (IRs) due to the inertia of the isolator are neglected. Previous research on the IR problem does not clarify all the characteristics of distributed parameter isolators. Furthermore, with the development of active vibration isolation, which can avoid the compromise in the choice of damping in conventional passive isolation systems, the effects of IRs in isolators on the control performance and stability for commonly used control strategies need to be quantified. In this study the effects of IRs on the control performance and stability of an absolute velocity feedback (AVF) control system are presented. A stability condition for AVF control system is proposed and a simple approach to stabilize the control system is studied. Experimental work to validate the theoretical results is also presented.

1. INTRODUCTION

A conventional passive isolation system consists of a compliant isolator positioned between the host structure and the equipment to be isolated, which can provide good isolation performance at high frequencies in the isolation region [1]. However, conventional vibration isolators are usually assumed to be massless for modelling purposes, which tends to overestimate the isolator performance because the IRs (also referred to as wave effects) due to the inertia of the isolator are neglected [2]. This is especially important for lightly damped metallic isolators, since the smaller the loss factor of the isolator the more significant are the wave effects [3]. The degradation effects of the IRs on vibration isolation have been noticed by many researchers and some efforts have been made to suppress the effects by applying a high damping material in parallel with the original isolator [4], inserting intermediate masses [5] or using dynamic vibration absorbers [6]. However, previous research on the IR problem is not particularly comprehensive, because it does not clarify all the characteristics of distributed parameter isolators. Furthermore, with the development of active vibration isolation, which can avoid the compromise in the choice of damping in conventional passive isolation systems [7], the effects of IRs in isolators on the control performance and stability for commonly used control strategies need to be quantified.

The aim of this paper is to analyze an active vibration isolation system under AVF control containing an isolator which is modelled as a distributed parameter system and investigate its performance and stability in reducing vibration transmission from a vibrating base to a mounted equipment structure. In Section 2 the theoretical model is described in terms of mobility and a stability condition for AVF control system is proposed. Experimental validation is given in section 3. Finally, the conclusions are presented in Section 4.

2. THEORETICAL ANALYSIS

A vibration isolation system containing a distributed parameter isolator is shown as represented in terms of equipment mobility Y_e , isolator impedance $\mathbf{Z_r}$ and base mobility Y_b in Figure 1. This

corresponds to an isolated equipment mounted on a host structure that possesses its own dynamics and is excited by an external force f . The displacement of the mounted equipment and base are given by x_e and x_b respectively. The isolator is represented by a finite elastic rod, which has an impedance matrix [8]:

$$\mathbf{Z_r} = \begin{bmatrix} Z_{11} & Z_{12} \\ Z_{21} & Z_{22} \end{bmatrix} = \begin{bmatrix} -jS\sqrt{E^*\rho}\cot(k_l^* L) & jS\sqrt{E^*\rho}/\sin(k_l^* L) \\ jS\sqrt{E^*\rho}/\sin(k_l^* L) & -jS\sqrt{E^*\rho}\cot(k_l^* L) \end{bmatrix} \quad \text{(Eq. 1)}$$

where L, S, E^* *and* ρ are the length, cross-sectional area, Young's modulus and density of the rod, respectively; to account for damping in the isolator, the Young's modulus is assumed to be complex, i.e. $E^* = E(1+j\eta_m)$, where η_m is the loss factor; $k_l^* \approx k_l(1-j\eta_m/2)$ is the longitudinal wave number, where $k_l = \sqrt{\rho/E}\,\omega$, and ω is angular frequency. A control actuator, which is in parallel with the isolator, reacts between the equipment and the base. The control force f_a which is proportional to the velocity of the equipment mass v_e is fed back with a gain $-h$, as shown in Figure 1.

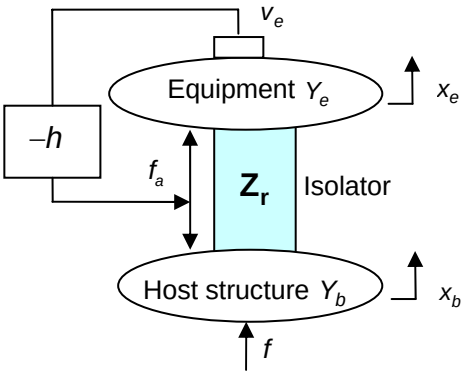

Figure 1.-Block diagram for a vibration isolation system containing a distributed parameter isolator under AVF control

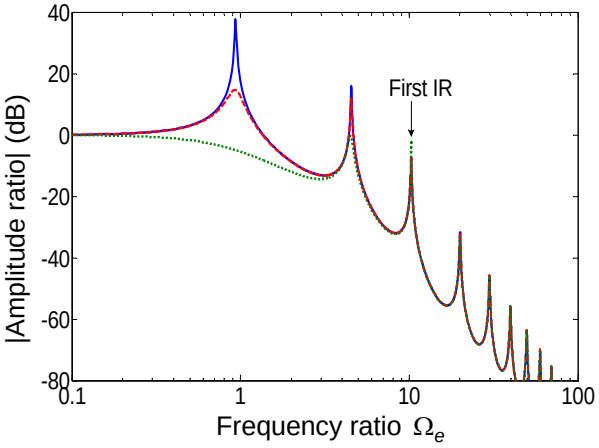

Figure 2.-Amplitude ratio of the vibration isolation system under AVF control when $\mu_m = 0.1$, $\mu_b = 0.5$, $\mu_k = 0.1$, $\eta_m = \eta_b = 0.01$ and $\zeta_a = 0$ (solid line), $\zeta_a = 0.1$ (dashed line), $\zeta_a = 1$ (dotted line), respectively

If the equipment has a mass-like mobility, i.e. $Y_e = 1/j\omega m_e$ and the base structure is modelled as a mass m_b on a complex spring, i.e. $k_b^* = k_b(1+j\eta_b)$, where η_b is the lost factor, the displacement amplitude ratio of the system under AVF control can be written as [3]:

$$\frac{x_e}{\delta_{st}} = \frac{k_b}{j\omega} \cdot \frac{Y_{eb}}{1+h(Y_{ee}-Y_{eb})} \quad \text{(Eq. 2)}$$

where $\delta_{st} = f/k_b$ is the static deflection of the base, Y_{ee} is the input mobility of the equipment when coupled to the rest of the system and Y_{eb} is the transfer mobility from the force on the base to the equipment velocity when the system is coupled. Letting $\Omega_e = \omega/\omega_e$, where $\omega_e = \sqrt{k_s/m_e}$ is the fundamental natural frequency, $k_s = ES/L$ is the static stiffness of the isolator, $\mu_m = \rho SL/m_e$ is the ratio of the mass of the isolator to that of the equipment, $\mu_k = k_s/k_b$ is the stiffness ratio, $\mu_b = m_b/m_e$ is the ratio of the mass of the base to that of the equipment and $\zeta_a = h/2\sqrt{k_s m_e}$ is the damping ratio due to AVF control, the amplitude ratio for the system under AVF control with different values of active damping ratio ζ_a is plotted in Figure 2. It can be seen that the resonance peak at the fundamental natural frequency of the mounted equipment is attenuated with an increase of the active damping ratio. The resonance peak at the natural frequency of the base, which is the second peak in Figure 2, is also attenuated if the

feedback gain is high. However, the IR peaks in the isolator are reduced much less, especially at relatively high frequencies, above the fundamental natural frequency, because the equipment mass dominates the response at these frequencies. Also it should be noted that some IR peaks inherent in the isolator, such as the third peak in Figure 2, are slightly amplified under AVF control which might cause the system to become unstable.

The plant response from the actuator force to the equipment velocity for this system is given by

$$G = Y_{ee} - Y_{eb} \quad \text{(Eq. 3)}$$

At a resonance frequency of a lightly damped isolation system, when only one mode dominates, the plant response can be written as:

$$G = Y_{ee} - Y_{eb} \approx \frac{\left[\phi_e^{(j)}\right]^2 \left(1 - \phi_b^{(j)} / \phi_e^{(j)}\right)}{2\sqrt{K_j M_j}\,\zeta_j} \quad \text{(Eq. 4)}$$

where $\phi_e^{(j)}$ and $\phi_b^{(j)}$ are the j^{th} mode shape evaluated at the equipment and base respectively, and K_j , M_j and ζ_j are modal stiffness, mass and damping ratio of the j^{th} mode with corresponding natural frequency $\omega_j = \sqrt{K_j / M_j}$. Based on the Nyquist criterion, for stability, one requires at a resonance frequency:

$$\phi_b^{(j)} / \phi_e^{(j)} < 1 \quad \text{(Eq. 5)}$$

i.e. $\left|\phi_b^{(j)}\right| < \left|\phi_e^{(j)}\right|$ if the mode shapes of the system evaluated at the equipment and base have the same phase. This provides a simple method to determine the stability of the system in terms of the mode shapes of the system. According to the definition of mode shapes $\phi_e^{(j)}$ and $\phi_b^{(j)}$, this stability condition means that if the displacement of the base is greater than the displacement of the equipment and these two displacements are in phase at the j^{th} natural frequency, then the system may become unstable. Therefore, to stabilize the control system the relative displacement of the base at the troublesome natural frequency needs to be altered. In some situations, this can simply be achieved by adding more damping in the isolator as discussed in [9]. More mass could also be added to the base structure to change the mode shape in order to stabilize the control system.

3. EXPERIMENTAL VALIDATION

A four-spring active vibration isolation system was built as shown in Figure 3. It consisted of an equipment plate together with four actuators mounted on a base plate through four springs under excitation of a primary vibrator. An aluminium plate ($160 \times 160 \times 10$mm) representing the equipment was installed symmetrically on top of another aluminium plate ($160 \times 160 \times 10$mm) representing the base via four identical helical springs, each of which had a mass of 27.1g and stiffness of 1.73×10^4N/m . A large electromagnetic vibrator underneath the base plate acted as the primary force actuator, and the four small electromagnetic actuators fixed on the equipment plate were the control actuators at each mount position. The equipment structure thus consisted of the aluminium equipment plate and four actuators which had a mass of 5kg. Each helical spring was bolted to the equipment plate through an aluminium washer underneath each actuator. A stinger was connected between each actuator and the washer at each spring foot through the inside of the spring. The base plate was fixed to the washers at each spring foot by wax and bolted to the primary vibrator with four bolts. The base structure had an effective mass of 1.18kg and effective stiffness of 4.25×10^4N/m .

To measure the open-loop frequency response, the four actuators fixed on top of the equipment plate were driven with the same white noise signal through a power amplifier, while the large vibrator was connected but inactive. The equipment acceleration responses were measured along two central lines (ten points evenly at each line) of the equipment plate by five accelerometers, and then passed through charge amplifiers to obtain velocity responses. The open-loop frequency response of the system was measured and averaged using the input to the power amplifier and the output from the charge amplifiers. The predicted and measured open-

loop frequency responses of the four-spring active vibration isolation system are shown in Figure 4(a). Apart from some differences in the resonant amplitudes, the theoretical results match fairly well with the experimental measurements, except for the unmodelled rotational modes around 32 Hz and 289 Hz, and the unmodelled flexural modal behaviour around 327 Hz and in the frequency range above 404 Hz. The data below 3 Hz had low coherence due to the low sensitivity in the instrumentation, so is not presented. The first IR in the helical springs was identified at around 404 Hz and compared well with predictions. The second IR was strongly coupled with some flexural modes in the equipment plate. The phase shift at low frequencies, where the phase is larger than 90º, is due to the phase advances in the power amplifier and charge amplifiers. The phase shift at high frequencies, where the phase tends to less than -90º, is due to the phase lag in the low pass filters incorporated inside the charge amplifiers.

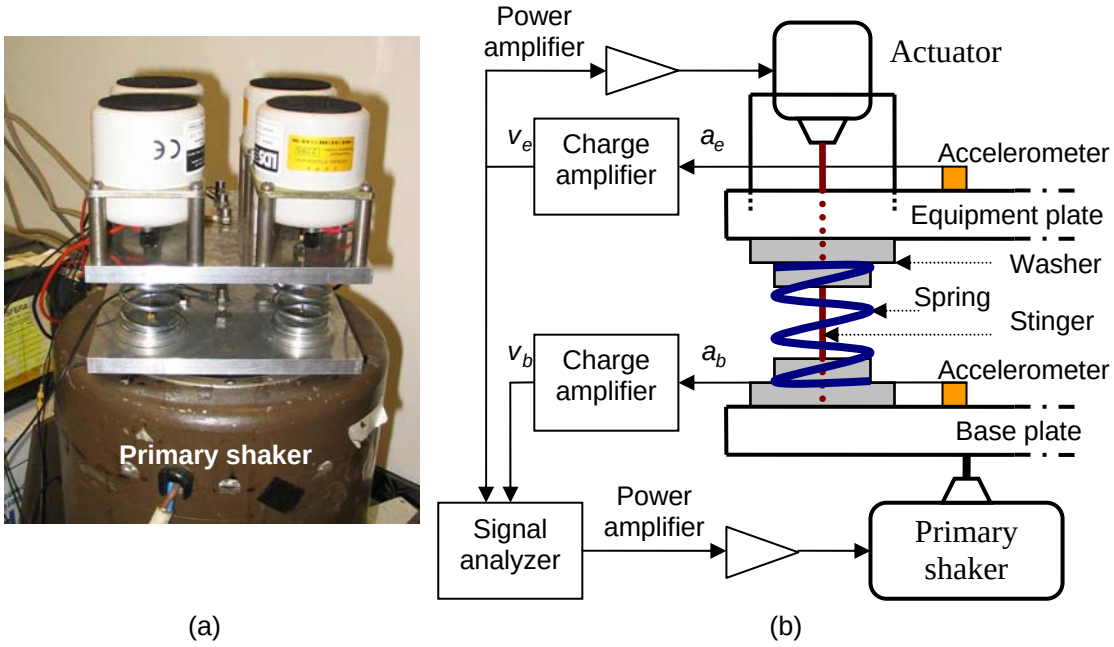

Figure 3.-(a) Photograph and (b) schematic diagram of one corner of the four-spring active vibration isolation system

The measured potential instability occurs at the first IR of the helical springs which forms a loop on the left hand side of the Nyquist plot in Figure 4(b). This supports the stability analysis in the theoretical study in Section 2 that the IRs may destabilize the AVF control system when the mass of the isolators becomes significant. The flexural mode in the equipment plate at 327 Hz also has a potential to destabilize the system, which is not considered in this study while it was mentioned by Kim et al [9]. The cause of the instability in the experiment also includes the phase advances in the power amplifier and charge amplifiers. The power amplifier has a phase advance up to about 90º at very low frequencies (under 5 Hz). Furthermore, an additional phase advance occurs in the charge amplifier. A phase advance of greater than 90º at very low frequencies can cause the Nyquist plot of the plant response to cross the negative real axis, and thus make the system unstable for a high gain. The two loops in the left half of the complex plane in Figure 4(b) crossing the negative real axis are caused by the flexural mode in the equipment plate at 327 Hz and the first IR in the helical springs at 404 Hz respectively. Also, the Nyquist plot of the plant response crosses the negative real axis at very low frequencies due to the phase advances in the power amplifier and charge amplifiers, which is not shown in Figure 4(b).

Based on the analysis in Section 2, one way to stabilize the system is to add mass to the base structure. Therefore, a mass of 1.8 kg was attached to the base plate to investigate whether this would stabilize the system. The measured open-loop frequency responses of the stabilized system are shown in Figure 5(a), where the original open-loop frequency responses are also shown for comparison. The base resonance was reduced to a lower frequency due to the attachment of the mass. The amplitude and phase of the first IR are also changed with the

phase lag being reduced from -235º to -175º. However, the flexural mode in the equipment plate at 327 Hz is not affected because the change of the base dynamics does not affect the flexural modal behaviour in the equipment plate. So adding mass to the base structure can eliminate the instability caused by the first IR in the isolator, but it has no effect on the instability caused by the flexural modal behaviour in the equipment plate. Figure 5(b) shows the Nyquist plot of the open-loop frequency response between 350 and 450 Hz where only the first IR occurs for the original and stabilized system. It can be seen that, for the stabilized system, the loop on the left half of the complex plane due to the first IR in the spring is shifted to the third quadrant rather than crossing the negative real axis.

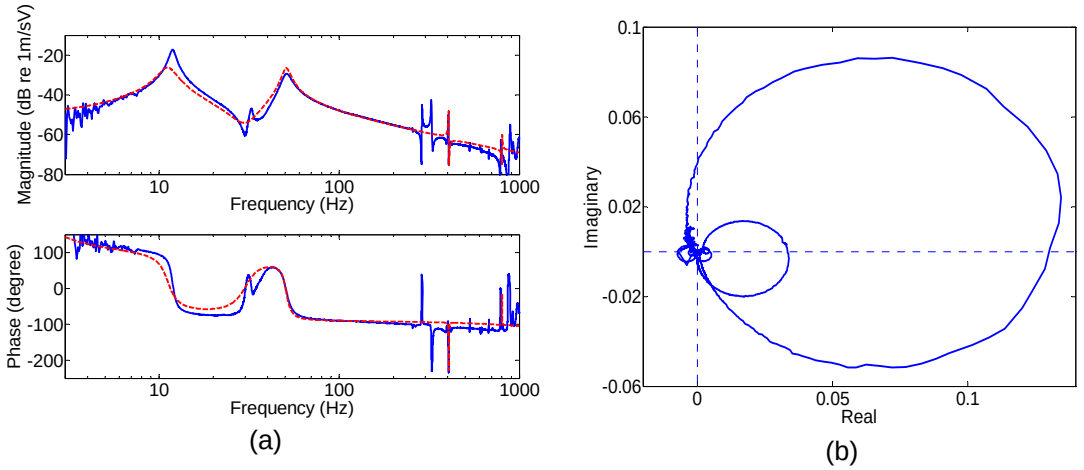

Figure 4.-(a) Measured (solid) and predicted (dashed) open-loop frequency response and (b) Nyquist plot of the open-loop frequency response of the active vibration isolation system

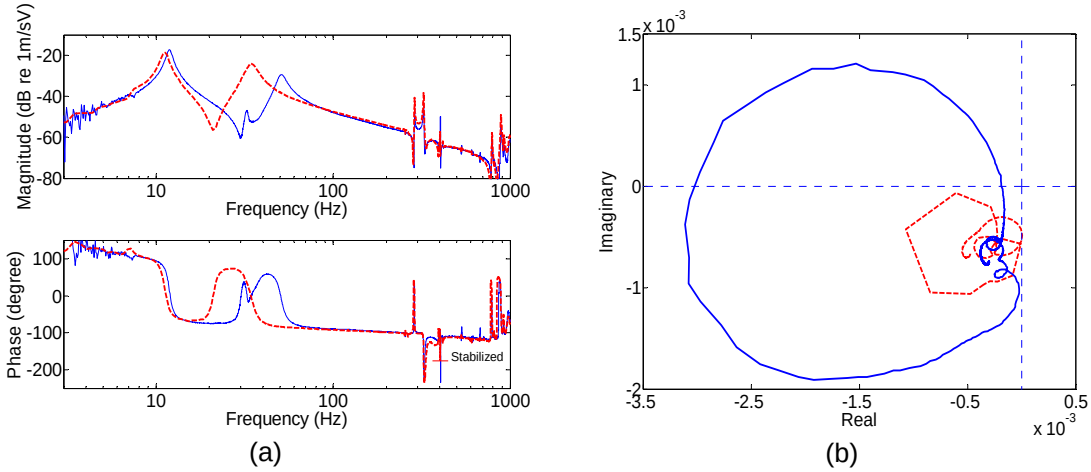

Figure 5.-(a) Measured open-loop frequency response and (b) Nyquist plot of the open-loop frequency response between 350 Hz and 450 Hz, for the original system (solid) and the stabilized system (dashed)

A single-channel absolute velocity feedback control was implemented on each of the four springs with the equipment structure mounted onto the base structure. The large vibrator was driven with white noise. The velocity responses of the equipment were also obtained with the response at the centre of the equipment plate fed back into four actuators through a power amplifier to generate the control forces. Each feedback channel had an equal, constant feedback gain. Figure 6 shows the velocity response of the equipment plate per unit voltage to the primary vibrator without control and with various control gains. The gain margin for the higher feedback gain used was 1.8 dB. The instability occurred firstly at low frequencies due to the phase advances in the high-pass filters incorporated in the charge amplifiers and power amplifiers [10]. Responses less than 3 Hz are again excluded from the plots. The resonance peaks at low frequencies, e.g. the equipment and base resonance peak are well attenuated as the control gain is increased. However, the resonance peaks at high frequencies including the first IR peak in the springs are not reduced because the mass of the equipment structure

dominates the response in this frequency range rather than the active damping. In fact there is a small increase in the amplitude at the first IR in the helical springs at 404 Hz. A similar amplification in the amplitude occurs around 327 Hz.

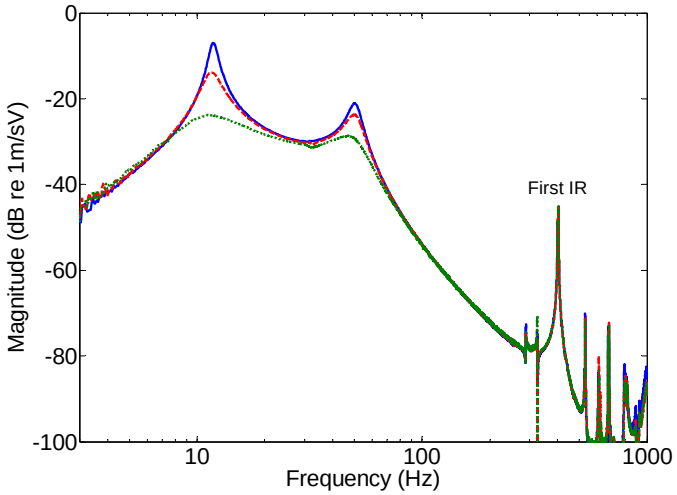

Figure 6.-Measured velocity response of the equipment plate per unit voltage to the primary vibrator of the active vibration isolation system with various feedback gains: without control (solid), low control gain (dashed) and high control gain (dotted).

4. CONCLUSIONS

The effects of IRs in distributed parameter vibration isolators on the control performance and stability of an AVF control system have been investigated theoretically and experimentally. AVF control is effective in reducing the resonance peaks at low frequencies, but it has little effect on the resonance peaks at relatively high frequencies, including the IR peaks in the isolators, because the equipment mass dominates the response in that frequency range. Furthermore the IRs in the isolators may destabilize the AVF control system. A stability condition based on the mode shapes of the system has been proposed. Based on the stability condition, it has been shown that the AVF control system can be stabilized by adding more mass onto the base structure.

References: [1] D. J. Mead: Passive Vibration Control, John Wiley & Sons, 1999
[2] M. Harrison, A. O. Sykes, M. Martin: Wave effects in isolation mounts. Journal of the Acoustic Society of America **24 (**1952) 62-71
[3] B. Yan, M. J. Brennan, S. J. Elliott, N. S. Ferguson: Velocity feedback control of vibration isolation systems, ISVR Technical Memorandum No. 962, University of Southampton, UK, 2006
[4] G. R. Tomlinson: Vibration Isolation in the Low and High Frequency Range, Mechanical Engineering Publication, Edmunds, Suffolk, England (1982) 21-29
[5] J. C. Snowdon: Vibration and Shock in Damped Mechanical Systems, Wiley, New York, 1968
[6] Y. Du, R. A. Burdisso, E. Nikolaidis, D. Tiwari: Control of internal resonances in vibration isolators using passive and hybrid dynamic vibration absorbers. Journal of Sound and Vibration **286** (2005) 697-727
[7] D. Karnopp: Active and semi-active vibration isolation. American Society of Mechanical Engineers Journal of Mechanical Design **177** (1995) 177-185
[8] P. Gardonio, M. J. Brennan: Mobility and impedance methods in structural dynamics, Chapter 9 in Fundamentals of Noise and Vibration, F. J. Fahy, J. G. Walker, ed., E&FN SPON, London, 1998
[9] S. M. Kim, S. J. Elliott, M. J. Brennan: Decentralized control for multichannel active vibration isolation. *IEEE Transaction on control systems technology* **9, No.1** (2001) 93-100
[10] M. J. Brennan, K. A. Ananthaganeshan, S. J. Elliott: Instabilities due to instrumentation phase-lead and phase-lag in the feedback control of a simple vibrating system, Journal of Sound and Vibration, In press